

# Functionalisation of ethylene–propylene copolymer by melt grafting of maleic anhydride using a high shear internal mixer

N. Mohamad<sup>\*1</sup>, M. A. Mahamood<sup>1</sup>, Y. Juliana<sup>1</sup>, A. R. Jeefferie<sup>1</sup>, A. Muchtar<sup>2</sup>, M. I. Shueb<sup>3</sup>, M. S. Kassim<sup>1</sup>, M. A. Azam<sup>1</sup>, Y. M. Yuhazri<sup>1</sup>, N. Mustafa<sup>1</sup>, A. R. Toibah<sup>1</sup>, T. R. Sahroni<sup>1</sup> and Q. Ahsan<sup>1</sup>

This study focused on synthesising a peroxide-initiated maleic anhydride-g-ethylene–propylene copolymer via melt grafting using a Haake internal mixer at high shear rate. The effect of maleic anhydride and dicumyl peroxide percentage on the grafting efficiency of maleic anhydride onto ethylene–propylene copolymer chains was carried out through a two-level factorial experimental design using Design Expert 6.0.5 software. The maleic anhydride and dicumyl peroxide content were varied, in the range of 1–5 and 0.1–0.3 phr, respectively. The grafting parameters were fixed at a temperature of 180°C and rotor speed of 60 rev min<sup>-1</sup> for 5 minutes. The grafting efficiency was determined by Fourier transform infrared spectroscopy analysis based on cumulative absorbance of anhydrides' characteristic peaks and supported by differential scanning calorimetry and field emission scanning electron microscopy analyses. The grafting was highly influenced by maleic anhydride and dicumyl peroxide content. The optimum functionalisation was achieved at 5 phr maleic anhydride and 0.3 phr peroxide addition.

**Keywords:** Ethylene–propylene copolymer (EPM), Melt functionalisation, Maleic anhydride, Grafting parameters, Rubber blends incompatibility

## Introduction

Blending of two or more polymers produces material with improved properties and better processability, making it superior to its original phases at minimal cost.<sup>1–3</sup> For instance, rubber blends are widely utilised in automobile parts such as springs and snubbers, hoses and belting, seals and bearings,<sup>4</sup> engine mounts,<sup>5</sup> gears gaskets, pneumatic tires and tubes.<sup>3</sup> Previous research works have reported some attractive elastomer blends such as natural rubber/ethylene–propylene diene monomer (NR/EPDM),<sup>6,7</sup> butadiene rubber/ethylene–propylene diene monomer (BR/EPDM),<sup>8</sup> nitrile–butadiene rubber/ethylene–propylene diene monomer (NBR/EPDM),<sup>7,8</sup> NR/BR/EPDM,<sup>9</sup> natural rubber/epoxidised natural rubber (NR/ENR),<sup>10</sup> NR/styrene BR (SBR)/BR,<sup>11</sup> natural rubber/butyl rubber (NR/IIR)<sup>12</sup> and natural rubber/ethylene–propylene copolymer (NR/EPM).<sup>1,13,14</sup> Among these blends, NR/EPDM shows great potential in outdoor applications because of its

excellent thermal, chemical and ozone resistance, as well as attractive dynamic properties.<sup>6,13</sup> For example, poor outdoor properties of high unsaturated rubbers such as NR can be significantly improved by the incorporation of EPDM without sacrificing their unique mechanical properties.<sup>9</sup>

According to Kothandaraman,<sup>2</sup> a successful NR/SBR blend may exhibit discrete areas of each elastomer in the range of ~0.5 μm.<sup>2</sup> However, in most cases elastomers are immiscible because of their high molecular weight chains, viscosity mismatch, differences in cure rates, different saturation levels and polarity mismatch.<sup>9,13</sup> Immiscibility produces blends with poor mechanical properties. Owing to that, compatibilisation is required to improve the compatibility of the blends.<sup>15</sup> In the findings of El-Sabbagh<sup>6</sup> and Zhang *et al.*<sup>9</sup>, the incorporation of a small amount of compatibiliser reduces the domain size of the dispersed phase, and thus enhances the compatibility and rheological properties of the blend.

Generally, compatibilisation can be conducted either physically or chemically. Physical compatibilisation is achieved by the addition of a third polymer into the elastomer's blend to form a block or grafted copolymers.<sup>6</sup> The third polymer acts as a surfactant where the high polar component of the blend will attract towards the high polar part of the compatibiliser and vice versa. The third polymer can be BR,<sup>6</sup> chlorinated rubber or SBR<sup>6</sup> and ENR.<sup>16,17</sup> According to Mohamad *et al.*,<sup>16</sup> ENR is

<sup>1</sup>Faculty of Manufacturing Engineering, Universiti Teknikal Malaysia Melaka, Durian Tunggal 76100, Melaka, Malaysia

<sup>2</sup>Faculty of Engineering and Built Environment, Universiti Kebangsaan Malaysia (UKM), Bangi 43600, Selangor, Malaysia

<sup>3</sup>Radiation Processing Technology Division, Malaysia Nuclear Agency, Bangi 43600, Selangor, Malaysia

\*Corresponding author, email noraiham@utem.edu.my

frequently used as a compatibiliser in producing NR nanocomposites because of its high polarity. On the other hand, chemical compatibilisation is achieved by the addition of a reactive or functional compound into the blends in order to induce *in situ* chemical reaction between the blends' components.<sup>18</sup> For chemical compatibilisation, maleic anhydride (MAH) from the vinyl monomers group is often used to be grafted onto a polymer either through free radical copolymerisation or melt grafting. The anhydride group will be grafted to polar polymer and forms a functionalised compound.<sup>2,14,15</sup> According to Stuart<sup>19</sup> and Segneanu *et al.*,<sup>20</sup> MAH grafting is identified by a distinctive carbonyl band region at several characteristic infrared bands: (1840–1800), (1780–1740) and (1300–1100)  $\text{cm}^{-1}$  which correspond to anhydrides stretching regions (–CO–O–CO–). In addition, a strong C–O stretching band of open-chain and cyclic anhydride structures may be observed near 1150  $\text{cm}^{-1}$  or ranging around 1150–1300  $\text{cm}^{-1}$ , respectively. Furthermore, based on Ismail and co-workers,<sup>21</sup> the grafting of MAH is also indicated by the presence of band at (1710–1719) and (1770–1792)  $\text{cm}^{-1}$ , which can be attributed to C = O symmetric stretching bonds. Examples of functionalised compatibiliser for EPDM-based blend are EPDM-g-PVAc,<sup>14</sup> MMA-g-EPDM,<sup>13</sup> EVA-g-MAH, mercapto-functionalised EVA, mercapto-modified EPDM and MAH-g-EPDM.<sup>9,22</sup>

Maleic anhydride-g-ethylene–propylene copolymer is a potential compatibiliser and is similar to MAH-g-EPDM in terms of structure except for the double bond. Referring to Zhang *et al.*,<sup>9</sup> addition of MAH-g-EPM in NR/BR/EPDM blends increases the chemical reactivity of the blends because of an increase in polarity of the EPDM. This is because of the presence of the MAH group, which provides extra polarity to the EPDM and is well linked to the high polar double bond of the NR diene rubber phase.

Melt compounding via internal mixer is a widely used technique for preparing polymer compounds and blends.<sup>17</sup> Uniform compounding is achieved when the materials are sheared between two rotors that are circulating in an opposite manner in the mixer chamber. High shear forces are needed for a blending process in order to overcome the high viscosity of melted elastomers.<sup>2</sup> Nevertheless, melt grafting via internal mixer is a rarely used technique to produce MAH-g-EPM compatibiliser. Normally, polymer functionalisation is carried out via solution mixing.<sup>23,24</sup>

This study is an effort to measure the efficiency of melt grafting through high shear melts compounded using a Haake internal mixer. It is aimed at preparing MAH-g-EPM via peroxide-initiated melt grafting of anhydride onto an EPM backbone as well as to detect the optimum formulation of MAH-g-EPM using a mathematical and statistical technique. Response surface methodology (RSM) is selected due to its being less time consuming and having the ability to detect the true optimum of the factor.<sup>25</sup> Incorporation of low molecular weight peroxide is expected to activate the inert polyolefin and thus induce functionalisation of EPM with MAH.

## Experimental

Ethylene–propylene copolymer with propylene content of 80%, melt flow index of 1.3 g per 10 minutes, and density

of 0.862  $\text{g cm}^{-3}$  was supplied by Exxon Mobil Chemical. Maleic anhydride ( $\text{C}_4\text{H}_2\text{O}_3$ ) with purity of 99% and average molecular weight,  $M_w$  of 98.06  $\text{g mol}^{-1}$  was supplied by Scharlau. Bis( $\alpha,\alpha$ -dimethylbenzyl)peroxide (DCP) as free radical initiator and crosslinking agent with purity of 98%,  $M_w$  of 27 037  $\text{g mol}^{-1}$  and density of 102  $\text{g cm}^{-3}$  was supplied by Merck.

Maleic anhydride-grafted EPM compounds were prepared by blending 100 phr EPM, 1–5 phr varied amount of MAH and 0.1–0.3 phr varied amount of DCP in a Haake internal mixer at a temperature of 180°C, rotor speed of 60  $\text{rev min}^{-1}$  and mixing period of 5 minutes. The internal mixer used was equipped with a Banbury-type rotor blade and a mixing chamber capable of 78  $\text{cm}^3$  volume, with fill factor of 0.70. Equation (1) was applied to calculate the total mass of ingredients capable by the mixing chamber

$$m_{\text{total}} = \rho \times V_{\text{chamber}} \times 0.7_{\text{fill factor}} \quad (1)$$

All the three components were initially dry-mixed in a weighing tray before being immediately introduced into the mixing chamber. The mixing was performed up to 5 minutes for a complete peroxide reaction and to produce a homogenous blend. The generated compounds were then conditioned for Fourier transform infrared (FTIR) analysis.

The experiment for this study implemented a two-level factorial design using Design Expert software. The two-level factorial design for two independent variables, with three replications at centre point leads to a total of seven sets of experiments. In this experiment, the contents of MAH and DCP were varied in the range of 1–5 and 0.1–0.3 phr, respectively; whereas the content of EPM was kept constant.

## Maleic anhydride grafting efficiency characterisation through FTIR spectroscopy

Maleic anhydride-g-ethylene–propylene copolymer thin films of 200–250  $\mu\text{m}$  thickness were prepared by compression moulding using laboratory hydraulic hot moulding. Machine parameters for hot pressing were set at 150°C temperature, 5 MPa (or equivalent to 51  $\text{kg cm}^{-2}$ ) pressure for 10 minutes. The films were then dried in an air drying oven for 10 hours at 75°C in order to draw off the unreacted MAH from the thin films. The possible interaction of MAH with EPM was determined using a JASCO FTIR 6100 spectrometer machine through a thin film-FTIR approach. The FTIR spectra were collected from the MAH-g-EPM thin films in the transmission mode, and were recorded in the range 2000–400  $\text{cm}^{-1}$  with a 4  $\text{cm}^{-1}$  resolution and 50 scans. The different functional groups and structural features present in the molecules of MAH-g-EPM absorbed energy at the characteristic frequencies. The intensity of absorption is the indication of the bond strength and structural geometry in the molecules.<sup>26</sup> In this experiment, the FTIR spectra were used to identify the functional groups present on the EPM backbone after the grafting. At least five different spectra were generated for every sample to ensure a high confidence level.

Previous research on anhydride grafting efficiency analysis was conducted through a qualitative approach, which is based on the presence or occurrence of new characteristic peaks.<sup>27,21</sup> However, for this study, the FTIR analysis has been conducted quantitatively whereby the internal standard method is applied on the recovered spectra in order to build an equation that can be used to quantify anhydride through standard calculation. The approach is based on Lambert-Beer law theory.<sup>11</sup>

After the grafting efficiency was confirmed and quantified by FTIR, the next evaluation on statistical reliability was then performed by the Design Expert Statistical software. Then, analysis of variance (ANOVA) was applied to show the statistical significance of the MAH grafting to the EPM. From the experimental findings, the effect of independent variables on the grafting efficiency was studied using a half-normal graph, effect-list and regression model.

### Morphological analysis using field emission scanning electron microscope (FESEM)

Scanning electron microscopy analysis was conducted on gold-coated fracture surfaces of NR, EPDM and NR/EPDM vulcanisate samples using a Zeiss EVO-50 FESEM machine at a magnification of  $300\times$ . This analysis was performed to prove the efficiency of MAH-EPM as a compatibiliser in improving interaction between the NR and EPDM phase in the NR/EPDM blend.

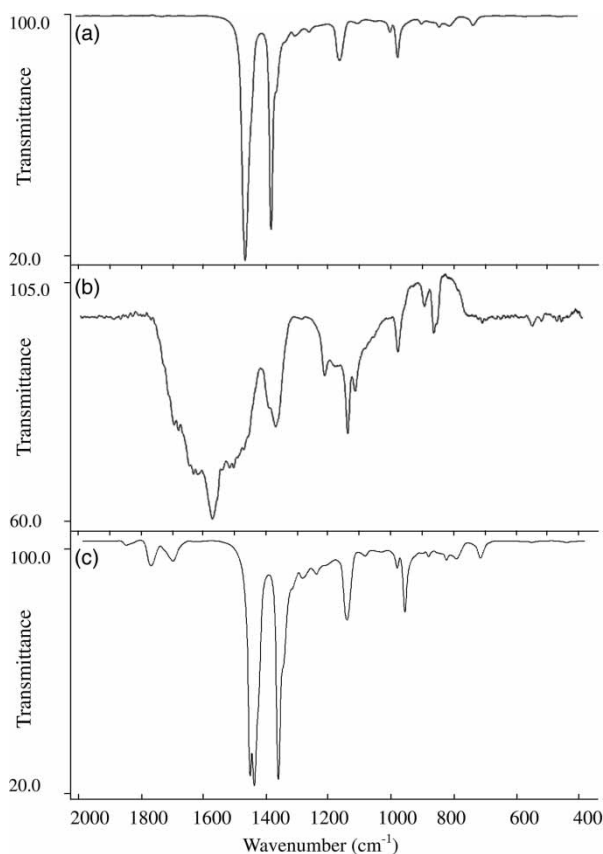
### Thermal analysis through differential scanning calorimetry (DSC)

Differential scanning calorimetry was conducted on NR, EPDM and NR/EPDM with/without MAH-EPM vulcanisates by heating the samples over the temperature range  $-65$  to  $160^\circ\text{C}$  at a heating and cooling rate of 10 and  $20^\circ\text{C}$  minute, respectively.

## Results and discussion

### FTIR-quantitative analysis of MAH-g-EPM

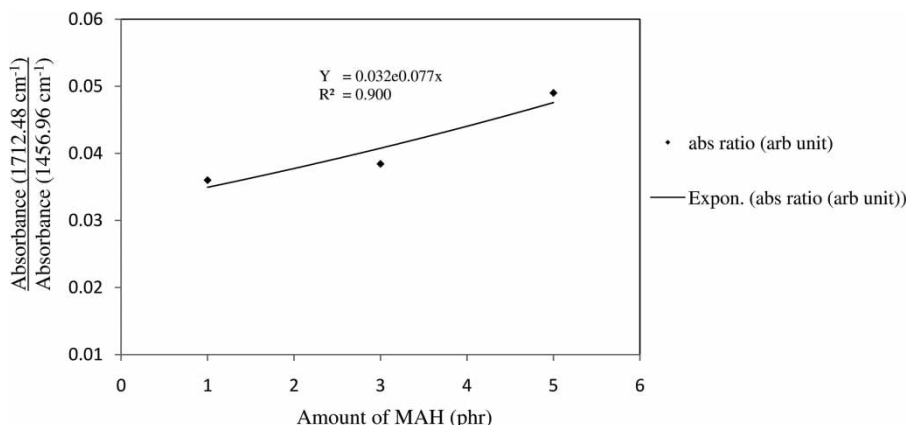
Figure 1 shows the FTIR spectra of pure EPM (spectrum A), maleic anhydride (spectrum B) and MAH-g-EPM (spectrum C) in the region of  $2000$ – $400\text{ cm}^{-1}$ . Referring to Fig. 1, there were obvious differences between infrared spectrum of MAH-g-EPM if compared to pure EPM as well as pure MAH. The MAH-g-EPM spectrum shows the presence of a few new peaks, increased absorbance in some MAH characteristic peaks and strong peaks and identification of an ethylene–propylene structure, except for minor broadening owing to peaks overlapping. By taking into consideration the increment of absorbance at typical anhydride characteristic peaks ( $1840$ – $1800$ ), ( $1780$ – $1740$ ), ( $1300$ – $1100$ ), ( $1710$ – $1719$ ) and ( $1770$ – $1792$ ),<sup>21,19,20,28</sup> the grafting of MAH onto EPM backbones was confirmed. However, it is important to ensure that the peak height of absorbance values for each selected band were measured by employing an appropriate baseline in order to get reliable and accurate infrared data.<sup>11</sup>



1 Fourier transform infrared spectra of a pure EPM, b pure MAH and c MAH-g-EPM

Based on the FTIR peak absorbance intensity data of each MAH-g-EPM sample, all samples exhibit an increment in intensity of anhydrides' characteristic peaks as compared to the peak intensity of pure MAH. It has been proved that the cumulative intensity of anhydride of all MAH-g-EPM samples increases in comparison with the absorbance intensity of the control/pure EPM sample. The increment demonstrated that all samples had experienced chemical modification and alteration in their respective functional groups. Owing to the utilisation of an absorbance ratio approach for quantitative grafting efficiency analysis, an internal standard is required to perform the quantification process; this approach follows the Lambert-Beer law theory.<sup>11</sup> Decision on an internal standard was referred to a selected range between  $1456$  and  $1460\text{ cm}^{-1}$  ( $6.85\text{ }\mu\text{m}$ ), where the intensity is at maximum  $\sim 99.00$ , referring to a strong band of polyethylene and polypropylene monomers of EPM rubber.

The anhydride content of MAH-g-EPM was then determined from the ratio of peaks heights of the absorbance peaks at  $1712.48$ – $1456.96\text{ cm}^{-1}$ , which correspond to anhydrides and polyethylene/polypropylene functional groups, respectively. Anhydrides' characteristic peak at the  $1712.48\text{ cm}^{-1}$  region was selected for the absorbance ratio approach because of its high confirmation of anhydride grafting based on the presence of a new peak on the MAH-g-EPM spectrum as compared to the pure EPM spectrum. Finally, a calibration curve of absorbance ratio ( $1712.48/1456.96\text{ cm}^{-1}$ ) v. MAH in phr was built and generated an exponential curve with



**2 Calibration curve using 1456.96 cm<sup>-1</sup> PE and PP vibration region as an internal standard**

$R^2 = 0.900$  (Fig. 2). There were only three points selected to represent the contribution of various MAH addition during the grafting process with EPM.

The amount of anhydride was then determined using equation (2), which has been derived from the  $Y$  and  $R^2$  values; and built from the exponential curve of the calibration curve:

$$\% \text{ Anhydride} = \frac{1}{0.077} \times \ln\left(\frac{A_{1712.48}/A_{1456.96}}{0.032}\right) \quad (2)$$

The MAH grafting efficiency as a function of MAH amount was calculated based on equation (2) and the result is shown in Table 1. Basically, the grafting efficiency mainly depends on the rate of MAH diffusion into the EPM phase. According to the data in Table 1, sample No. 1, with the formulation of 5 phr MAH and 0.3 phr DCP contributes to the highest percentage of anhydride grafting percentage compared to other MAH-g-EPM samples. When samples Nos. 1 and 7 are compared, it is clear that the optimum DCP level is crucial to lead to an efficient grafting mechanism. Insufficient initiator to activate the grafting process resulted in a non-grafting process that took place in sample No. 7 even though at a very high level of MAH content.

**Regression model of the functionalisation of MAH into EPM using RSM**

The experimental result was further proved by RSM statistical tools. By selecting a significant model term from ANOVA, a regression model for grafting yield  $Y$  (equation (3)) and an effect list were generated. By using the equation (3), the predicted grafting yield at each experimental point was obtained. This result was supported by the effect list (as shown in Table 2), which stated the variable  $B$  to be the most significant factor with 88.02% contribution to grafting yield than 0.37% contribution by variable  $A$ .

$$Y = 2.91 - 0.14A + 2.14B + 0.62AB \quad (3)$$

Analysis of variance calculates values such as mean of square (MS), sum of square (SS),  $F$  value,  $P$  value and

coefficient of multiple determinations ( $R^2$ ). Variable  $B$  and the interaction point  $AB$  were selected as significant model terms because their  $P$  values were lower than 0.05. Variable  $A$  was not significant because its  $P$  value was greater than 0.10, which indicates the term is not significant. Even though variable  $A$  was not significant, it cannot be eliminated because the interaction point  $AB$  provides a significant model term. This model was accurate and can be used to navigate the design space because it shows a high  $R^2$  value of 0.9960. The  $R^2$  value implies that the sample variation of 99.60% for the grafting efficiency was attributable to the variables being tested. It also indicates that only 4.74% of the total variation was not explained by the model.

The selection of the best grafting formulation was finally conducted based on the highest grafting yield using the selected regression model. First, a combination was chosen because it has the highest desirability of 1.00. The optimum grafting efficiency was obtained at 5 phr MAH and 0.3 phr DCP at grafting yield of 5.54%.

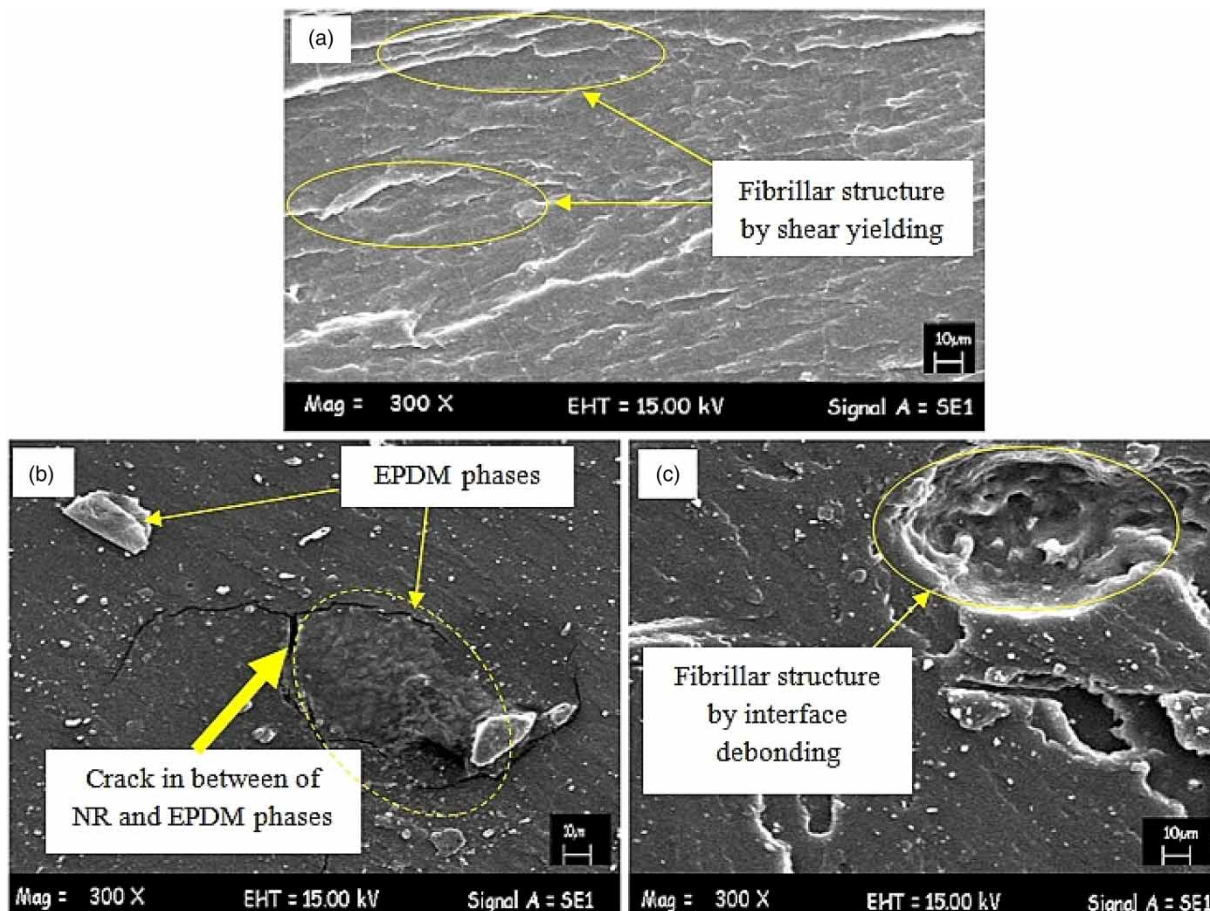
**Table 1 Anhydride grafting percentage as a function of MAH and DCP contents in the grafting formulation**

Sample no.	MAH content (phr)	DCP (phr)	Relative peak height* at 1712.48 (cm <sup>-1</sup> )	Anhydride grafting (%)
1	5	0.3	4.89	5.54
2	3	0.2	3.82	2.38
3	3	0.2	3.81	2.32
4	1	0.3	4.54	4.57
5	3	0.2	3.66	2.00
6	1	0.1	3.59	1.53
7	5	0.1	1.33	0.00

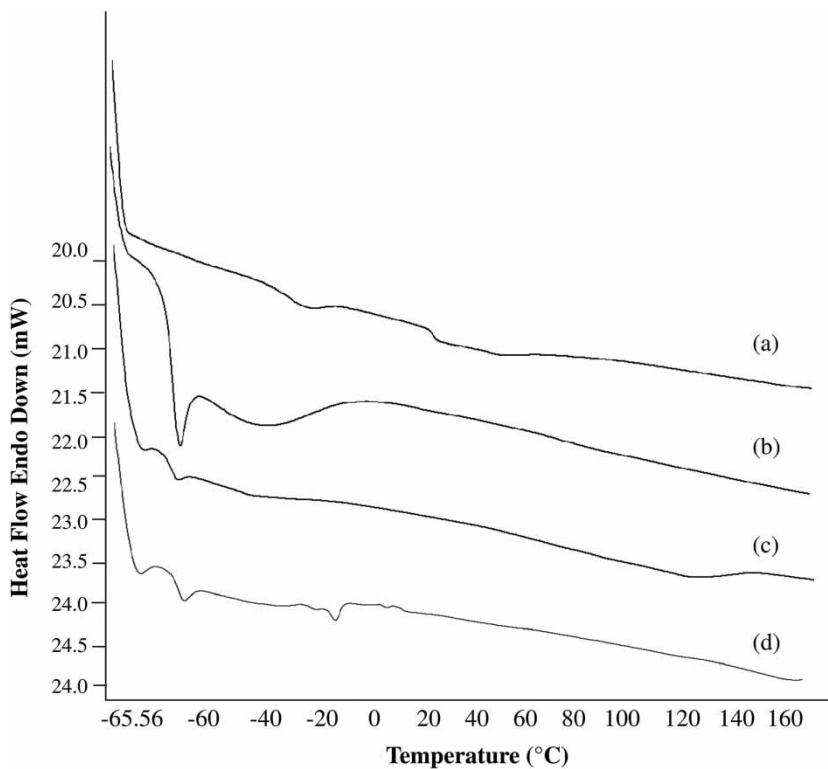
\*Relative to that of the 1456.96 cm<sup>-1</sup> peak.

**Table 2 Effect list of all model terms for the screening experiments**

Term	Sum of square (SS)	F-value	P-value	Percentage of contribution (%)
A	0.078	1.92	0.3002	0.37
B	18.40	452.19	0.0022	88.02
AB	1.56	38.28	0.0251	7.45



3 Scanning electron microscopy micrographs showing tensile fracture surface of a NR, b NR/EPDM without MAH-EPM and c NR/EPDM with MAH-EPM



4 The endothermic curves of a NR, b EPDM, c NR/EPDM with MAH-EPM and d NR/EPDM without MAH-EPM

## Morphological characteristics

The SEM analyses of NR/EPDM blends were conducted to visualise the miscibility between NR/EPDM blends with the presence of MAH-EPM as compatibiliser. The tensile fracture surfaces of NR vulcanisate and NR/EPDM blends are shown in Fig. 3. In Fig. 3a, NR exhibits high surface roughness, indicated by the fibrillar structure because of shear yielding mechanism. The fibrillar structure is an indication of ductile fracture, which shows high tensile strength of natural rubber vulcanisate. Figure 3b shows a relatively smooth surface of NR/EPDM blend without MAH-EPM, which represents a higher degree of brittleness induced by the incorporation of EPDM in NR. Furthermore, there is an obvious interface crack between NR and EPDM phases (shown by thick arrow in Fig. 3b) because of mismatch in molecular movement of their chains during the tensile deformation. In contrast, an improvement in ductility is observed with the presence of MAH-EPM in the NR/EPDM blend (Fig. 3c). It is exhibited by occurrence of shear yielding and interface debonding mechanisms on the fracture surface. The homogeneously blended 30 phr EPDM in 70 phr NR matrix caused the blend to be dominated by NR ductile behaviour. The ductile behaviour of NR is indicated by the fibrillar structures on the fracture surface. Hence, it is proven that MAH-EPM synthesised from 5 phr MAH and 0.3 phr DCP was successfully acting as compatibiliser for the rubber blend.

## Thermal analysis

The glass transition temperature ( $T_g$ ) is an indirect representation of the heterogeneous nature of NR/EPDM blends. A single and sharp peak indicates a highly miscible blend. Meanwhile, an intermediate peak with a value between those of the constituent components shows a partial miscible blend and separated peaks indicate an immiscible blend. In Fig. 4, endothermic curves of NR vulcanisate (Fig. 4a) and EPDM vulcanisate (Fig. 4b) exhibit single  $T_g$  peak with the value of  $-1.8$  and  $-51.2$ , respectively. However, this was shifted to  $-51.3$  in the NR/EPDM blend with the presence of MAH-EPM (Fig. 4c) as compatibiliser. This single peak indicates a miscible blend and the least distinct  $T_g$  indicates reasonable interaction between the blend components. Moreover, two separated  $T_g$  peaks at  $-50.7$  and  $-11.1$  in NR/EPDM without compatibiliser (Fig. 4d) proved the low miscibility of the blend.

## Conclusion

Maleic anhydride -g-ethylene-propylene copolymer has been successfully prepared by the melt compounding procedure of ethylene-propylene copolymer, maleic anhydride and dicumyl peroxide. Fourier transform infrared spectroscopy-quantitative data indicate that the highest percentage of anhydride grafting was achieved with the grafting formulation of 5 phr maleic anhydride and 0.3 phr dicumyl peroxide. This finding was in good agreement with the optimisation result obtained from the analysis of variance statistical results conducted using response surface methodology. Based on the analysis of variance experimental finding through half-normal plot and effect list, it shows that both variables, variable  $A$  (maleic anhydride amount) and variable  $B$  (dicumyl

peroxide amount), were significant model terms that contributed to grafting efficiency. However, the dicumyl peroxide amount was the most significant variable with highest percentage of contribution (88.02%) and sum of squares, SS (18.40). According to  $R^2 = 0.9960$  derived from analysis of variance, the model was significant and attributable to the studied variables. The potential of maleic anhydride-ethylene-propylene copolymer compound to promote miscibility in the natural rubber/ethylene-propylene copolymer blend is evident from its morphological and thermal properties.

## References

1. M. Arroyo, M. Lopezmanchado, J. Valentin and J. Carretero: 'Morphology/behaviour relationship of nanocomposites based on natural rubber/epoxidized natural rubber blends', *Comput. Sci. Technol.*, 2007, **67**, 1330-1339.
2. B. Kothandaraman: 'Rubber materials', 2008, India, Ane Books.
3. W. D. Callister: 'Material science and engineering: an introduction', 2007, New York, John Wiley & Sons.
4. A. N. Gent: 'Engineering with rubber: how to design rubber components', 2001, Cincinnati, Hanser.
5. J. G. Sommer: 'Engineered rubber products: introduction to design, manufacture, and testing', 2009, Cincinnati, Hanser.
6. S. H. El-Sabbagh: 'Compatibility study of natural rubber and ethylene-propylene diene rubber blends', *Polym. Test.*, 2003, **22**, 93-100.
7. B. G. Soares, A. S. Sirqueira, M. G. Oliveira, M. S. M. Almeida and R. D. Janeiro: 'The reactive compatibilization of EPDM-based elastomer blends', *Raw Mater. Appl.*, 2002, **55**, 454-459.
8. M. Kharazmkia, G. Naderi, M. H. R. Ghoreishy and S. Shokoochi: 'Elastomer nanocomposites based on BR/EPDM/organoclay', *Rubber Chem. Technol.*, 2013, **86**, 299-312.
9. H. Zhang, R. N. Datta, A. G. Talma and J. W. M. Noordermeer: 'Maleic-anhydride grafted EPM as compatibilising agent in NR/BR/EPDM blends', *Eur. Polym. J.*, 2010, **46**, 754-766.
10. I. R. Gelling: 'Epoxidised natural rubber', *J. Nat. Rubber Res.*, 1991, **6**, 184-205.
11. Y. S. Lee, W. K. Lee, S. G. Cho, I. Kim and C. S. Ha: 'Quantitative analysis of unknown compositions in ternary polymer blends: a model study on NR/SBR/BR system', *J. Anal. Appl. Pyrolysis*, 2007, **78**, 85-94.
12. N. Suma, R. Joseph and K. E. George: 'Improved mechanical properties of NR/EPDM and NR/Butyl blends by precuring EPDM and Butyl', *J. Appl. Polym. Sci.*, 1993, **49**, 549-557.
13. W. Arayaprane and G. L. Rempel: 'Properties of NR/EPDM blends with or without methyl methacrylate-butadiene-styrene (MBS) as a compatibilizer', *Mater. Struct. Reliab.*, 2007, **5**, 1-12.
14. A. I. Hussain, M. L. Tawfic, A. A. Khalil and T. E. Awad: 'High performance emulsified EPDM grafted with vinyl acetate as compatibilizer for EPDM with polar rubber', *Nat. Sci.*, 2010, **8**, 348-357.
15. C. E. Koning, M. Van Duin, C. Pagnoulle and R. Jerome: 'Strategies for compatibilization of polymer blends', *Progr. Polym. Sci.*, 1998, **23**, 707-757.
16. N. Mohamad, A. Muchtar, M. J. Ghazali, D. H. Mohd and C. H. Azhari: 'Correlation of filler loading and silane coupling agent on the physical characteristics of epoxidized natural rubber-alumina nanoparticles composites', *J. Elastom. Plast.*, 2010, **42**, 331-346.
17. N. Mohamad, A. Muchtar, M. J. Ghazali, D. H. J. Mohd and C. H. Azhari: 'Epoxidized natural rubber - alumina nanoparticle composites: optimization of mixer parameters via response surface methodology', *Solid State Sci. Technol.*, 2009, **17**, 133-143.
18. J. L. White and K. J. Kim: 'Thermoplastic and rubber compounds: technology and physical chemistry', 2008, Cincinnati, Hanser.
19. B. Stuart: 'Infrared spectroscopy: fundamentals and applications', 2004, Chichester, John Wiley & Sons.
20. A. E. Segneanu, I. Gozescu, A. Dabici, P. Sfirloaga and Z. Szabadi: in 'Organic compounds FT-IR spectroscopy', in 'Macro to nano spectroscopy', (ed. J. Uddin); 2012, Europe, Intech.
21. P. Pasbakhsh, H. Ismail, M. N. A. Fauzi and A. Bakar: 'Influence of maleic anhydride grafted ethylene propylene diene monomer (MAH-g-EPDM) on the properties of EPDM nanocomposites reinforced by halloysite nanotubes', *Polym. Test.*, 2010, **28**, 548-559.
22. A. S. Sirqueira and B. G. Bluma: 'The effect of mercapto- and thioacetate-modified EPDM on the curing parameters and mechanical

- properties of natural rubber/EPDM blends', *Eur. Polym. J.*, 2003, **39**, 2283–2290.
23. Y. Promdum, P. Pairote and J. Ruamcharoen: 'Grafting copolymerization of natural rubber with 2-hydroxyethyl methacrylate for plywood adhesion improvement', *Songklanakarín J. Sci. Technol.*, 2009, **31**, 453–457.
  24. Z. M. O. Rzavey: 'Graft copolymers of maleic anhydride and its isostructural analogues: high performance engineering materials', *Int. Rev. Chem. Eng.*, 2011, **3**, 153–215.
  25. N. Mohamad, A. Muchtar, M. J. Ghazali, D. H. J. Mohd and C. H. Azhari: 'Epoxidized natural rubber – alumina nanoparticle composites: optimization of mixer parameters via response surface methodology', *J. Appl. Polym. Sci.*, 2009, **115**, 183–189.
  26. N. Mohamad: 'The effect of filler on epoxidised natural rubber-alumina nanoparticles composites', *Eur. J. Sci. Res.*, 2008, **24**, 538–547.
  27. G. Socrates: 'Infrared and Raman characteristic group frequencies: tables and charts', 3rd edn; 2004, UK, Wiley.
  28. O. P. Grygorivera and J. Karger-Kocsis: 'Melt grafting of maleic anhydride onto an ethylene propylene diene terpolymer (EPDM)', *Eur. Polym. J.*, 2000, **36**, 1419–1429.